

Supporting Information

Severin et al. 10.1073/pnas.0910216107

SI Text

Materials and Methods Liposomes. Single-membrane liposomes were prepared from asolectin (10 mg/ml) in a solution containing 10 mM Tris-HCl (pH 7.4), 100 mM KCl, and 100 mM CF. The mixture containing multi- and single membrane liposomes was passed through a Nucleopore filter with 0.1 μm holes by means of an Avanti Polar Lipid Extruder. Then single membrane liposomes were passed through Sephadex G-50 to remove external CF. Efflux of CF from liposomes was measured fluorometrically (490 nm excitation, 520 nm emission) using a Fluorate Panorama fluorimeter (Lumex). Inside liposomes, the fluorescence was quenched due to stacking of CF occurring at high CF concentration. When appearing outside liposomes, CF fluorescence strongly increased due to dilution of CF, resulting in decomposition of the stacking structures. In certain experiments, doxorubicin substituted for CF (inner concentration, 30 mM; excitation, 450 nm; emission, 590 nm).

Isolation of yeast mitochondria. Yeast mitochondria were obtained from *D. magnusii* strain VKM Y261. The *D. magnusii* cells were cultivated in agitated Erlenmeyer flasks in batches of 100 mL in glycerol-containing medium at 28°C. Cells were harvested at the late exponential growth phase (10–13 g wet weight/L). Mitochondria were isolated from the cells washed twice with ice-cold water, resuspended (0.1 g wet cells/mL) in 50 mM Tris-HCl buffer, pH 8.6, containing 4 mM dithiothreitol, and incubated at room temperature for 10–15 min. Then the cells were pelleted at 3,000 g for 10 min, washed twice with ice-cold water to remove excess dithiothreitol, and incubated at 28°C under gentle stirring for 15–20 min in 10 mM HEPES-buffer, pH 7.2, containing 1.1 M sorbitol and 3 mg of Zymolyase 20T from *Arthrobacter luteus* (ICN Biomedicals) and 30 mg helicase per g of original cells (wet weight) to form spheroplasts. Spheroplast formation was monitored by measuring the osmotic fragility of a 100- μl sample of the cell suspension after a 1:10 dilution in distilled water. The spheroplasts were rapidly cooled, pelleted by centrifugation at 1,000 g for 10 min, washed twice with 1.1 M sorbitol containing 5 mM MgSO_4 (pH 7.2), resuspended (0.1 g wet cells/mL) in 10 mM Tris-HCl buffer (pH 7.2) containing 0.4 M mannitol, 0.5 mM EDTA, 0.5 mM EGTA, and BSA (4 mg/mL), and disrupted in an all-glass Dounce homogenizer (Kontes, Vineland, NJ, USA) with a low clearance pestle. The homogenate was mixed with an equal volume of the same buffer, except that 0.4 M mannitol was substituted by 0.6 M mannitol, and centrifuged at 1,200 g for 10 min. The supernatant was centrifuged once more at 7,000 g for 20 min. The resulting pellets from the second centrifugation were gently resuspended in 20 mL washing medium (EDTA, EGTA, and BSA were excluded), recentrifuged at 6,000 g for 20 min, and resuspended in a minimal volume of the washing medium. The mitochondrial preparations showed respiratory control values ranging from 5 to 8 (incubation medium, 0.6 M mannitol, 0.2 mM Tris-phosphate (pH 7.2–7.4), 20 mM Tris-succinate, 24 μM safranin O, and mitochondria, 0.5 mg protein/mL).

Molecular dynamics. We used NAMD 2.6 (1) for running MD simulations and the Adaptive Biasing Force (ABF) method (2) for modeling the potentials of mean force (PMF). The temperature was maintained with the Berendsen thermostat using a coupling parameter of 5ps^{-1} . The pressure was maintained at 1 atm by the Langevin piston method with piston mass of 100 atomic mass unit and Langevin collision frequency of 50ps^{-1} . Non-bonded

interactions were computed using the particle mesh Ewald method with 10 Å real space cutoff for electrostatic interactions and the switching functions between 10 and 12 Å for the vdW. The multiple time-step method was employed for the electrostatic forces; the non-bonded interaction list was constructed using a cutoff of 14 Å, updated every 40 steps. The covalent bonds involving hydrogen atoms were constrained using the SHAKE algorithm (MD integration step size, 1 fs).

The lipid and water molecules were modeled with the CHARMM27 all-hydrogen lipid force field (2) and the TIP3P model (4), respectively. The molecular force field parameterization for C_{12}TPP was obtained by combination of the standard CHARMM27 parameters for phenyl rings with parameters determined *de novo* by *ab initio* calculations using the PC-GAMESS program (5). The equilibrium distances and angles were found by DFT calculations which were performed with B3LYP functional and Pople 6-31G split valence basis set; partial charges of atoms were calculated by electrostatic potential fitting at a Connolly grid.

Molecular dynamics simulations were performed in the *NPT* ensemble at $T = 320$ K and pressure 1 atm. After the initial 25 ns equilibration, the average box size was $41.5 \times 47.8 \times 53.7$ Å³ (membrane plane perpendicular to z -axis), the area A per lipid being 66.2 Å². The MD simulations for the ABF calculations were initiated by dragging either the phosphorus atom of C_{12}TPP or the carbonyl atom of palmitate from the bulk on the positive half of the z -axis toward the bilayer center. We used 11 beads covering the z -coordinate range of -22.0 to 22.0 Å, with the coordinate origin located at the membrane center. Each bead had 4.0 Å length and was split into 20 bins (0.2 Å each) where the PMFs were calculated after accumulation of 50,000 samples in a bin prior to application of the ABF MD simulation in each bead continued for 10 ns, the total ABF simulation time being 110 ns.

Results In the first experiments, we used BLMs as model membranes. Addition of either SkQ1 or C_{12}TPP to the incubation mixture resulted in generation of $\Delta\psi$ across the BLM formed from *E. coli* phospholipids if there was a pH gradient between two BLM-separated compartments (more acidic compartment was negatively charged, Fig. 2A). The generated $\Delta\psi$ values were always smaller than 40 mV, never reaching theoretical (Nernstian) potential, i.e., 60 mV per pH unit. Tetraphenylphosphonium (TPP) containing phosphonium cation but, in contrast to SkQ1, no decane linker and plastoquinone was also competent in this effect, however the $\Delta\psi$ values generated even at the 1,000-fold higher TPP concentration were about three-fold smaller than with SkQ1. As to decylplastoquinone, modeling the other part of the SkQ1 molecule, it was quite ineffective. Fig. S2B shows that acidification of the medium resulted in formation of $\Delta\psi$ of opposite direction than alkalization. The effect of 1 mM TPP was completely abolished by micromolar concentration of bovine serum albumin (BSA). A similar effect of BSA was also observed with SkQ1, but in this case it might be explained by stoichiometric binding of SkQ1 by BSA, an explanation excluded in the case of TPP added at very much higher concentration than BSA. When these experiments were performed, it was already known that TPP facilitates the uncoupling effect of fatty acids on mitochondria (22, 23). This is why we suggested that protonophorous action of SkQ1 and C_{12}TPP on BLMs might be mediated by contaminations of free fatty acids in samples of the *E. coli* phospholipids. To avoid such contaminations, we substituted synthetic diphytanoylphosphatidylcholine (DPPC) for bacterial phospholipids, but this did not abrogate $\Delta\psi$

generation. Then we purified our DPPC sample from anionic contaminations using Ambersep-300 just before use and found that this procedure strongly decreased the ΔpH -supported $\Delta\psi$ generation. Direct measurement of phytanic acid concentrations in the DPPC samples showed that there were 0.05–0.1 and 0.02 μg DPPC/ml before and after the Ambersep-300 treatment, respectively. The $\Delta\psi$ values correlated with the free phytanic acid con-

tent. Addition of 20 μM palmitate to the incubation mixture strongly increased $\Delta\psi$ generated across a BLM that was formed from the purified DPPC (Fig. S2C). A control experiment showed that a ‘‘canonical’’ protonophorous uncoupler trifluoromethoxy-carbonylcyanide phenylhydrazone (FCCP) generated Nernstian ΔpH -dependent $\Delta\psi$ in a fatty acid- and penetrating cation-independent fashion.

1. Phillips JC, et al. (2005) Scalable molecular dynamics with NAMD. *J Comput Chem* 26:1781–1802.
2. Henin J, Chipot C (2004) Overcoming free energy barriers using unconstrained molecular dynamics simulations. *J Chem Phys* 121: 2904–2914.

3. Feller SE, Gawrisch K, MacKerell AD, Jr. (2002) Polyunsaturated fatty acids in lipid bilayers: intrinsic and environmental contributions to their unique physical properties. *J Am Chem Soc* 124:318–326.
4. Jorgensen WL, Chandrasekhar J, Madura JD, Impey RW, Klein ML (1983) Comparison of simple potential functions for simulating liquid water. *J Chem Phys* 79:926–935.

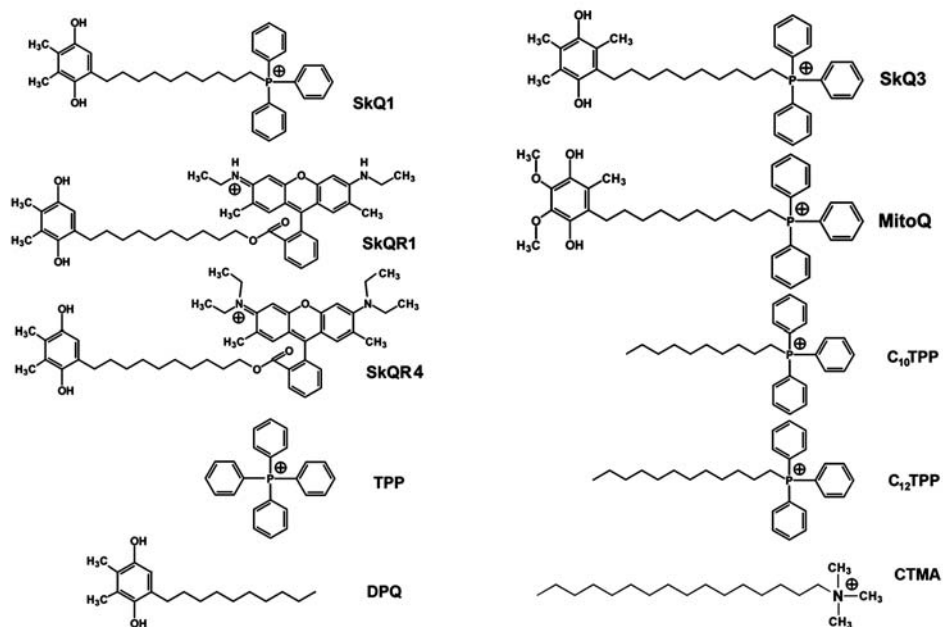


Fig. S1. Formulas of the synthesized cations.

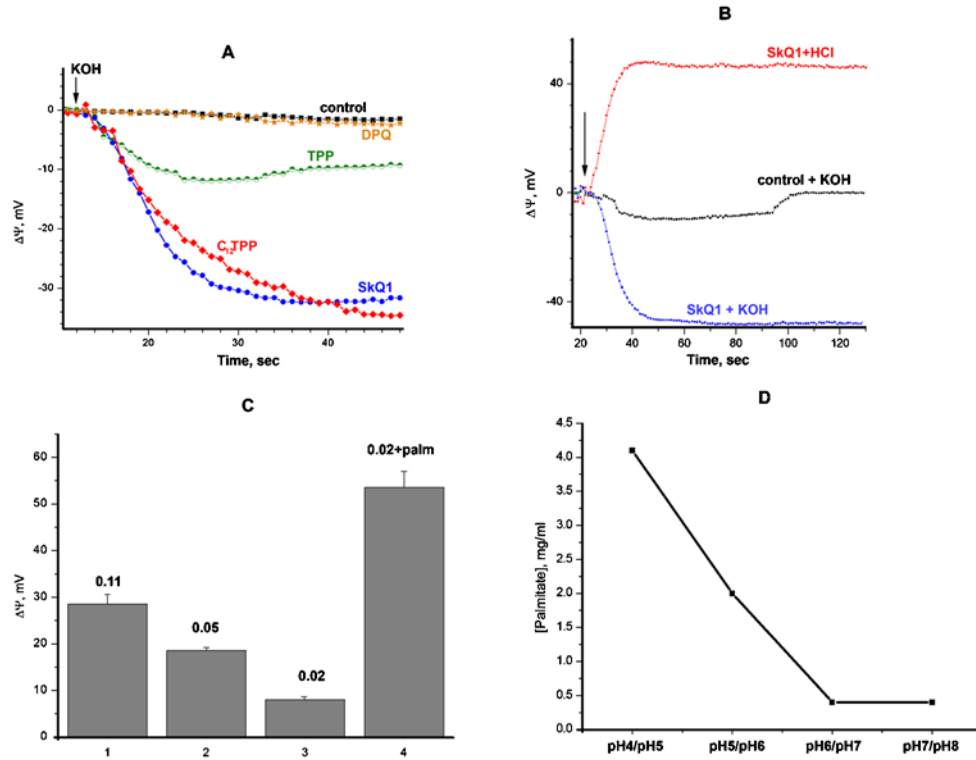


Fig. S2. Effects of SkQ1, C_{12} TPP, and SkQR1 on BLM (A–F) and liposomes (G, H). (A, B) A BLM was formed from *E. coli* phospholipids. Electric potential difference across the BLM ($\Delta\psi$) is assumed to be generated due to protonophorous effect of fatty acid contamination in the sample of phospholipids. Where indicated, $1 \mu\text{M}$ SkQ1, C_{12} TPP, or decylplastoquinone (DPQ) was added. In (A), KOH was added to the incubation mixture (10 mM KCl, 10 mM Tris, and 10 mM MES) to obtain pH 7.0; addition of KOH to one of the BLM-separated compartments (arrow) shifted pH in this compartment to 8.0. In (B) the pH of the incubation mixture (50 mM Tris and 10 mM KCl, pH 7.5) was shifted to 8.5 or 6.5 by adding KOH or HCl, respectively. (C) A BLM was formed from synthetic diphytanoylphosphatidylcholine (DPPC). (C, column 1) DPPC stored as a powder; (C, column 2) DPPC stored in chloroform solution; (C, column 3) as (C2) but the DPPC was purified from contamination of phytanic acid, using Ambersep-300; (C, column 4) as (C3) but $20 \mu\text{M}$ palmitate was added to the incubation mixture composed of 10 mM Tris, 10 mM KCl, pH 7; the pH was shifted to 8.0 by addition of KOH; numbers above columns, phytanic acid contamination, μg DPPC/mL. (D) Amount of palmitate required to generate half-maximal (30 mV) $\Delta\psi$ per ΔpH of 1 unit as a function of pH; for incubation mixture, see C. (E) $\Delta\psi$ value as a function of [SkQ1]; pH was shifted in one component from 7 to 8 by adding KOH; incubation mixture, 10 mM Tris, 10 mM KCl. (F) A palmitate-induced increase in electric current through a BLM formed from *E. coli* phospholipids; where indicated, $20 \mu\text{M}$ palmitate was added to both compartments; incubation mixture, $0.5 \mu\text{M}$ SkQR1, 0.1 M KCl, 10 mM Tris, pH 7.4; at zero time, 100 mV $\Delta\psi$ was applied to the BLM (G, H). Single membrane liposomes were loaded with 100 mM CF (G, black curve, and H) or 30 mM doxorubicin (G, red curve). Additions, 5×10^{-7} M SkQR1 and 0.25 μg melittin/mL (G); 2.5×10^{-7} M SkQR1, 2×10^{-5} M palmitate (palm) and 0.1% Triton X100. Incubation mixture, in case of liposomes loaded by CF, 0.1 M KCl, 10 mM Tris, pH 7.4; in case of liposomes loaded by doxorubicin, 0.1 M KCl, 10 mM MES, pH 6.0.

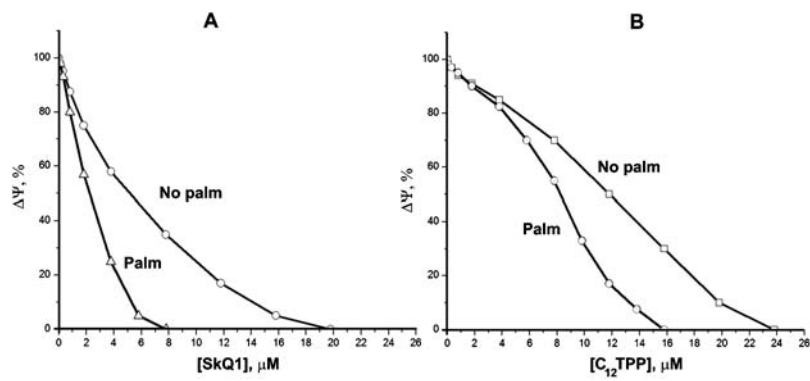


Fig. S4. Effect of SkQ1 (A) and C₁₂TPP (B) on $\Delta\Psi$ in rat heart mitochondria

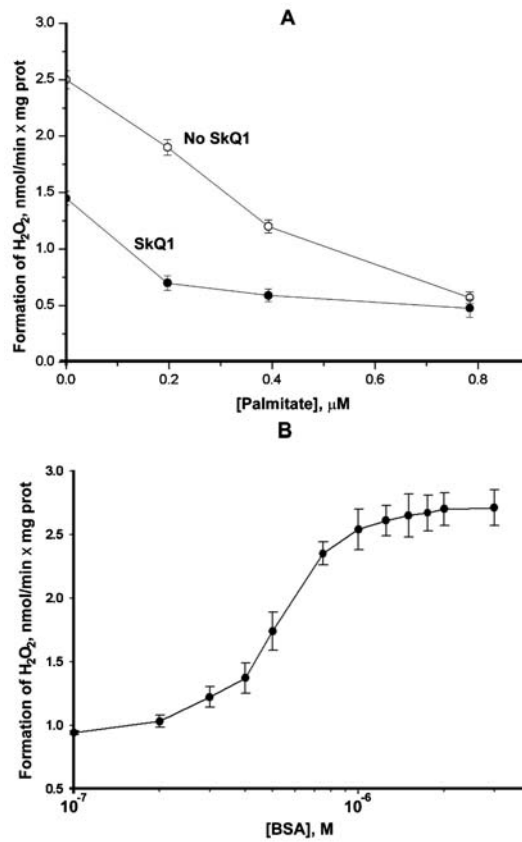


Fig. S5. Effects of palmitate, SkQ1, and BSA on H₂O₂ generation by rat heart mitochondria. For conditions, see Fig. 3C.

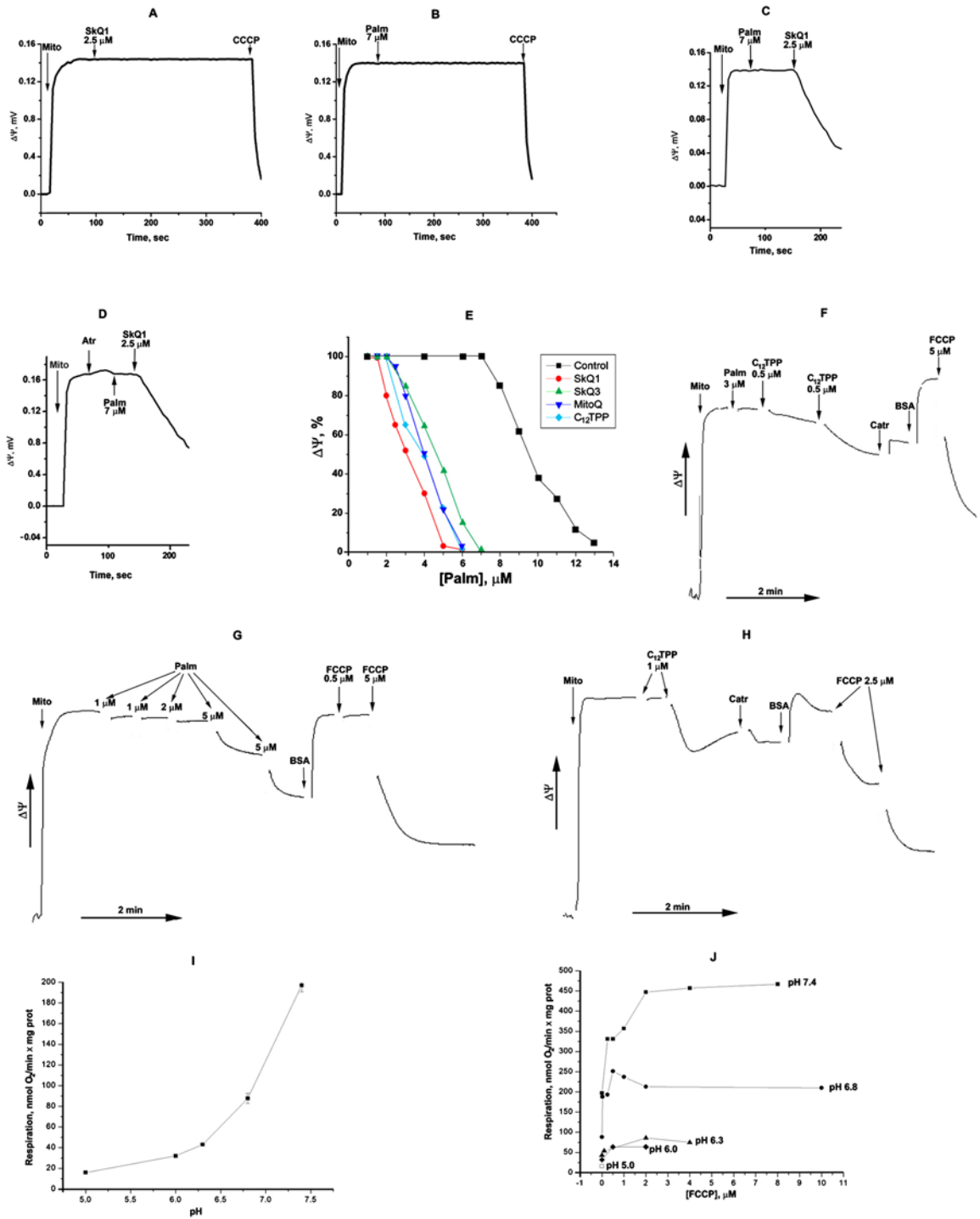


Fig. S6. Effect of SkQ1 and related compounds on mitochondria isolated from yeast *Dipodascus magnusii* (A–E) or *Saccharomyces cerevisiae* (F–J). (A–E) Incubation mixture, 0.6 M mannitol, 0.2 mM Tris-phosphate (pH 7.2), 0.5 mM EGTA, 20 mM succinate, and 10.5 μ M safranin O. Additions, mitochondria (0.5 mg protein/ml), 2.5 μ M (A–D) or 1.5 μ M (E) SkQ1, 7 μ M palmitate (A–D), 25 nM CCCP (A–C), 50 μ M atractylate (Atr) (D), 1.5 μ M SKQ3 (E), 1.5 μ M MitoQ (E), 2.5 μ M C₁₂TPP (E). (F–J) Incubation mixture, 0.6 M mannitol, 10 mM tris-HCl, 2 mM potassium phosphate, pH 7.4, 6.8, or 6.0, 4 mM pyruvate and 1 mM malate.

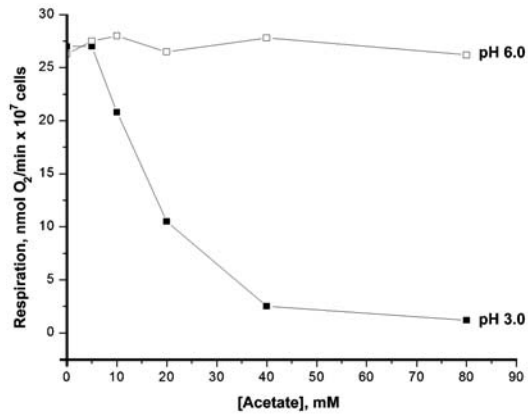


Fig. S7. Acetate inhibits respiration of *S. cerevisiae* cells at low pH. For conditions, see Fig. 4.

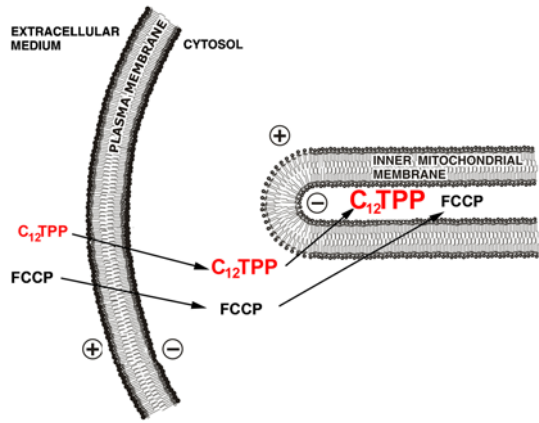
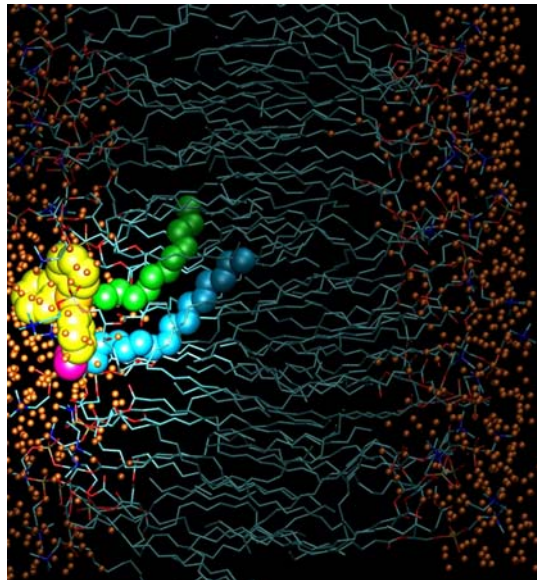


Fig. S8. A scheme illustrating that $C_{12}TPP$, but not FCCP, accumulates inside mitochondria.



Movie S1. A movie illustrating transmembrane diffusion of the $C_{12}TPP$ /palmitate ion pair. Molecular dynamics revealed interesting details in the very beginning of ion pair translocation. It is seen in the movie that the process starts with a “dancing” of the penetrating cation in the hydrophobic phase in the vicinity of charged palmitate carboxyl, the latter still remaining almost motionless in the interface. An impression arises that the cation tries to pull the anion out from the interface and to shift it to the hydrophobic region of the membrane. Apparently, such a “dancing” in the hydrophobic region becomes possible since $C_{12}TPP$ is not only very hydrophobic, but its positive charge is strongly delocalized. This means that the cationic group of $C_{12}TPP$ can easily move from the interface to the hydrophobic membrane core. This is not the case for CTMA. Its charged group, like that of palmitate, is always in the interface and therefore cannot pull palmitate out from the interface to the hydrophobic membrane core. This is apparently why CTMA does not substitute for SkQ1 or $C_{12}TPP$ as a palmitate carrier (see Fig. 1B). [Movie S1 \(AVI\)](#)